

Компьютерная модель распространения звука в легких

А. А. Родионов | 1 к маг.
н/р Я. А. Туровский | к. мед. н., доцент

Цель работы

Цель работы

- Разработать комп. модель распространения звука в легких.

Цель работы

- Разработать комп. модель распространения звука в легких.
- Изучить поведение звука, эффекты при различных условиях.

Задачи работы

Задачи работы

1. Анализ литературы

Задачи работы

1. Анализ литературы
2. Основывать модель на реальных данных

Задачи работы

1. Анализ литературы
2. Основывать модель на реальных данных
3. Математическая модель

Задачи работы

1. Анализ литературы
2. Основывать модель на реальных данных
3. Математическая модель
4. Компьютерная модель

Задачи работы

1. Анализ литературы
2. Основывать модель на реальных данных
3. Математическая модель
4. Компьютерная модель
5. Графический интерфейс для управления параметрами модели

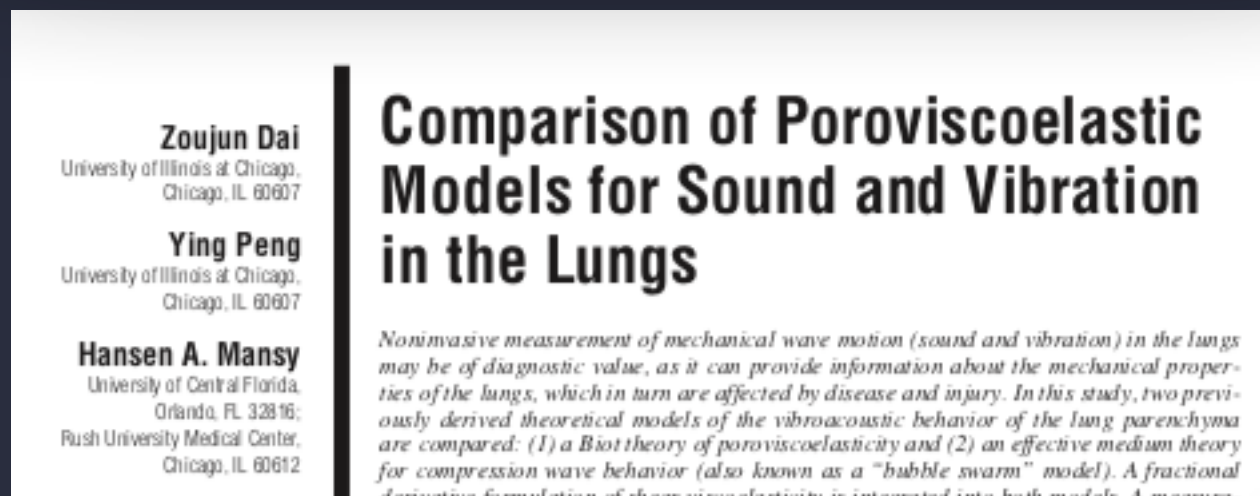
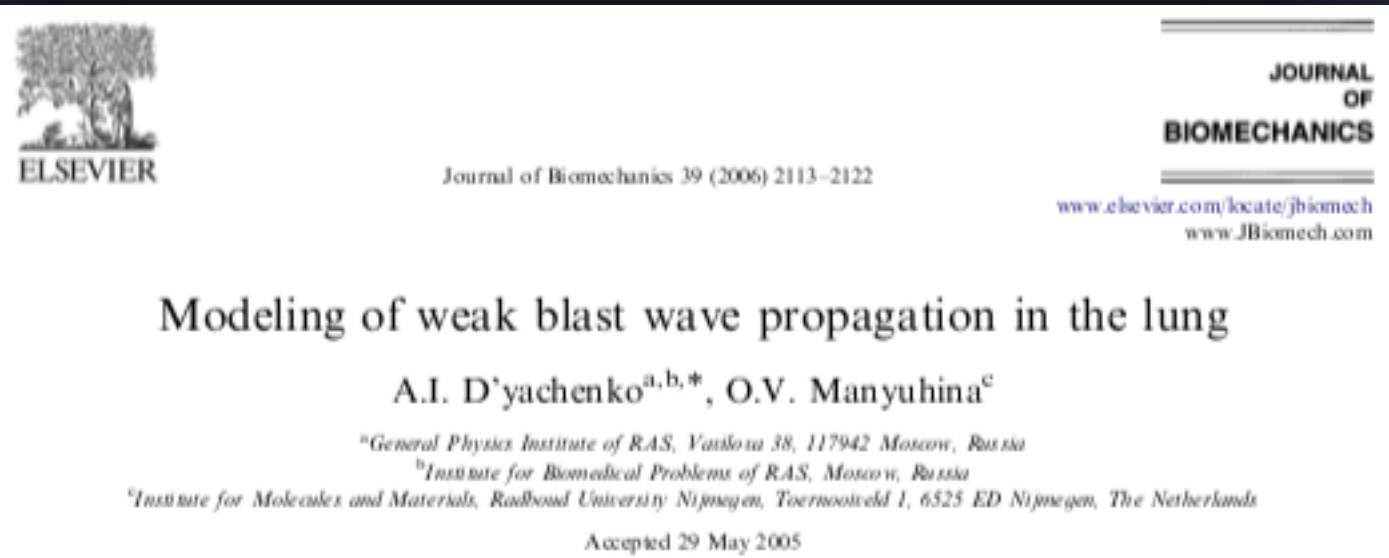
Задачи работы

1. Анализ литературы
2. Основывать модель на реальных данных
3. Математическая модель
4. Компьютерная модель
5. Графический интерфейс для управления параметрами модели
6. Оптимизация модели для SIMD, GPU, CUDA

Задачи работы

1. Анализ литературы
2. Основывать модель на реальных данных
3. Математическая модель
4. Компьютерная модель
5. Графический интерфейс для управления параметрами модели
6. Оптимизация модели для SIMD, GPU, CUDA
7. Изучение эффектов модели

Анализ литературы



A comprehensive computational model of sound transmission through the porcine lung

Zoujun Dai^{a)}

Department of Bioengineering, University of Illinois at Chicago, Chicago, Illinois 60607

Ying Peng

Department of Mechanical and Industrial Engineering, University of Illinois at Chicago, Chicago, Illinois 60607

Brian M. Henry

Department of Bioengineering, University of Illinois at Chicago, Chicago, Illinois 60607

Hansen A. Mansy

MULTISCALE MODEL. SIMUL.
Vol. 13, No. 1, pp. 43-71

© 2015 Society for Industrial and Applied Mathematics

HOMOGENIZATION OF A MODEL FOR THE PROPAGATION OF SOUND IN THE LUNGS*

PAUL CAZEAUX[†], CÉLINE GRANDMONT[†], AND YVON MADAY[‡]

Abstract. In this paper, we are interested in the mathematical modeling of the propagation of sound waves in the lung parenchyma, which is a foam-like elastic material containing millions of air-filled alveoli. In this study, the parenchyma is governed by the linearized elasticity equations, and the air by the acoustic wave equations. The geometric arrangement of the alveoli is assumed to be periodic with a small period $\varepsilon > 0$. We consider the time-harmonic regime forced by vibrations induced by volumic forces. We use the two-scale convergence theory to study the asymptotic behavior as ε goes to zero and prove the convergence of the solutions of the coupled fluid-structure problem to the solution of a linear-elasticity boundary value problem.

4D FEM models of the human thorax

Ander Biguri and Manuchehr Soleimani

Engineering Tomography Lab (ETL), Electronic and Electrical Engineering, University of Bath, Bath, UK,
a.biguri@bath.ac.uk

Abstract: In order to be able to further study 3D EIT lung image in figure 2. This FEM models then are saved using imaging and to analyse if the movement of the lungs during the breathing cycle can be reconstructed, accurate FEM models of the whole breathing cycle are needed. In this the EIDORS data structure. The models have around 300K elements each.

Respiratory Medicine (2011) 105, 1396–1403



available at www.sciencedirect.com

ScienceDirect

journal homepage: www.elsevier.com/locate/rmed



Computerized lung sound analysis as diagnostic aid for the detection of abnormal lung sounds: A systematic review and meta-analysis

Arati Gurung^a, Carolyn G. Scraftford^b, James M. Tietzsch^b, Orin S. Levine^b

MULTISCALE MODELLING OF SOUND PROPAGATION THROUGH THE LUNG PARENCHYMA *

PAUL CAZEAUX^{1,2} AND JAN S. HESTHAVEN³

Abstract. In this paper we develop and study numerically a model to describe some aspects of sound propagation in the human lung, considered as a deformable and viscoelastic porous medium (the parenchyma) with millions of alveoli filled with air. Transmission of sound through the lung above 1 kHz is known to be highly frequency-dependent. We pursue the key idea that the viscoelastic parenchyma structure is highly heterogeneous on the small scale, and use two-scale homogenization techniques

Анализ литературы

State of the Art

Respiratory Sounds Advances Beyond the Stethoscope

HANS PASTERKAMP, STEVE S. KRAMAN, and GEORGE R. WODICK

Department of Pediatrics and Child Health, University of Manitoba, Winnipeg, Manitoba
School of Electrical and Computer Engineering, Purdue University, West Lafayette, Indiana

ISSN 1067-7710, Acoustical Physics, 2013, Vol. 59, No. 6, pp. 709–716. © Pleiades Publishing, Ltd., 2013.
Original Russian Text © A. D. Shiryayev, V. I. Korenbaum, 2013, published in Akusticheskiy Zhurnal, 2013, Vol. 59, No. 6, pp. 759–767.

ACOUSTICS OF LIVING SYSTEMS. BIOLOGICAL ACOUSTICS

Frequency Characteristics of Air-Structural and Structural Sound Transmission in Human Lungs

A. D. Shiryayev^a and V. I. Korenbaum^{a, b}

^a Il'ichev Pacific Oceanological Institute, Far East Branch, Russian Academy of Sciences,
ul. Baltiyskaya 43, Vladivostok, 690041 Russia
e-mail: v-kor@poi.dvo.ru

^b Far East Federal University, ul. Sukhanova 8, Vladivostok, 690091 Russia
Received September 14, 2012

Abstract—From an independent sampling of data on luminal probing of the lungs of 20 people, based on an analysis of the phase characteristics of the coherency function of the signal with linear frequency modulation in a frequency band of 80–1000 Hz recorded above the trachea and different areas of the chest, the frequency selectivity of the structural and air-structural transmission variants has been revealed. It has been established that structural sound transmission on average is observed in a band from 100 to 280 Hz and air-structural propagation lies in the frequency range from 100 to 500–700 Hz. Over areas of the lungs characterized by the presence of aerated tissues (the apex and lower lobe), more frequently there is air-structural transmission, whereas in the vicinity of dense organs of the mediastinum (intercapsular region), on the contrary, structural propagation dominates.

УДК 534.7

МОДЕЛИРОВАНИЕ ПРОЦЕССА РАСПРОСТРАНЕНИЯ ЗВУКА В ГРУДНОЙ КЛЕТКЕ ЧЕЛОВЕКА. ЧАСТЬ 2. АНАЛИЗ АКУСТИЧЕСКИХ СВОЙСТВ В НОРМЕ

И. В. ВОВК*, Л. И. КОСОВЕЦ*, В. Т. МАЦЫПУРА**, В. Н. ОЛИЙНЫК*

*Институт гидромеханики НАН Украины, Киев

**Киевский национальный университет имени Тараса Шевченко

A Numerical Model to study Auscultation Sounds under Pneumothorax conditions

Sridhar Ramakrishnan, Student Member, IEEE, Satish Udpa, Fellow, IEEE, and Lalita Udpa, Fellow, IEEE



PERGAMON

Computerized Medical Imaging and Graphics 26 (2002) 237–246

www.elsevier.com/locate/compmmed

Computerized
Medical Imaging
and Graphics

A computer model of lung morphology to analyze SPECT images

Jeffry D. Schroeter^a, John S. Fleming^b, Dongming Hwang^c, Ted B. Martonen^{d,e,*}

^aCurriculum in Toxicology, University of North Carolina, Chapel Hill, NC 27599, USA

^bDepartment of Nuclear Medicine, Southampton General Hospital, Southampton SO16 6YD, UK

^cMicroelectronics Division, IBM Corporation, Research Triangle Park, NC 27709, USA

^dNational Health and Environmental Effects Research Laboratory, Experimental Toxicology Division, US Environmental Protection Agency,
Research Triangle Park, NC 27711, USA

^eDivision of Pulmonary Diseases, Department of Medicine, University of North Carolina, Chapel Hill, NC 27599, USA

Received 1 February 2001; accepted 13 January 2002



PERGAMON

Computers in Biology and Medicine 31 (2001) 499–511

www.elsevier.com/locate/comphomed

Computers in Biology
and Medicine

Computer simulations of lung airway structures using data-driven surface modeling techniques

Richard M. Spencer^a, Jeffry D. Schroeter^b, Ted B. Martonen^{c,d,*}

^aLockheed Martin, US EPA Scientific Visualization Laboratory, Research Triangle Park, NC 27711, USA

^bCurriculum in Toxicology, University of North Carolina, Chapel Hill, NC 27599, USA

^cExperimental Toxicology Division, National Health and Environmental Effects Research Laboratory,
US Environmental Protection Agency, Mail Drop 74, Research Triangle Park, NC 27711, USA

^dDivision of Pulmonary Diseases, Department of Medicine, University of North Carolina, Chapel Hill,
NC 27599, USA

Анализ литературы

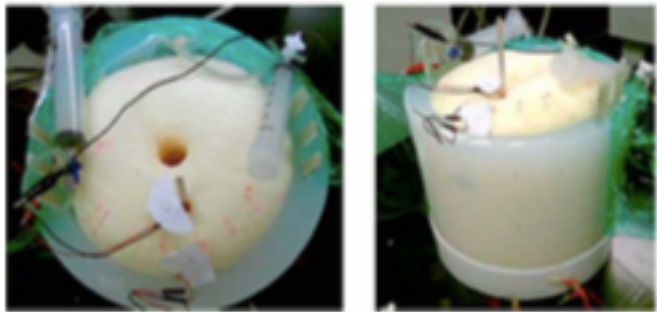
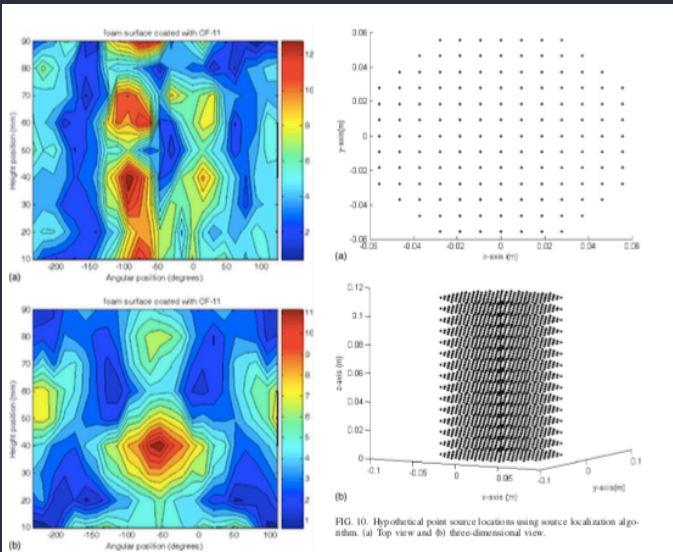


Fig. 6 Photograph of lung and chest wall mechanical phantom. Top and side views. Images show syringes that are used for inputting air into the bladders.

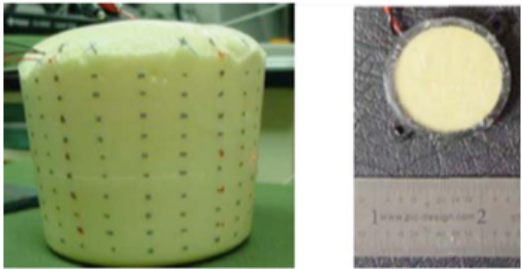


FIG. 5. (Color online) Lung measurement points and (right) volume mesh of lung with airway tree: (a) With airway network 1, (b) with airway network 2.

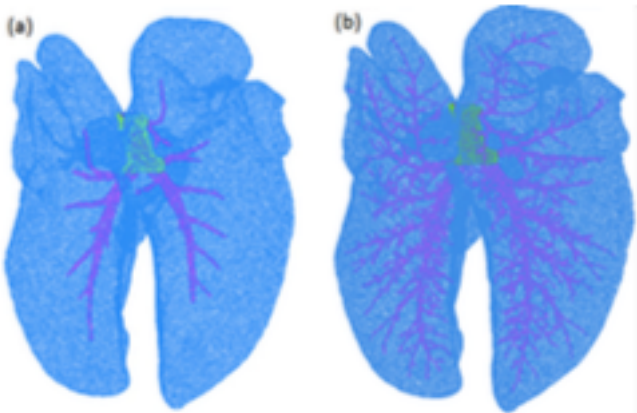


FIG. 5. (Color online) Volume mesh of lung with airway tree: (a) With airway network 1, (b) with airway network 2.

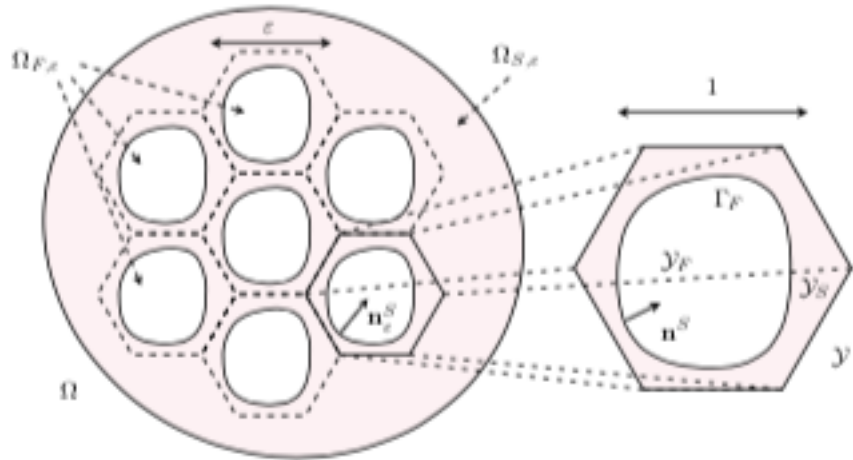


FIGURE 1. Domain Ω and reference cell \mathcal{Y} .

the whole space. The standard example is $\mathcal{Y} = (-1/2, 1/2)^d$ and $\mathbf{Z} = \mathbf{Z}^d$. We can also study, for example, a honeycomb as presented in Figure 1, where \mathcal{Y} is a hexagon with side $a > 0$ such that its volume is 1 and \mathbf{Z} the discrete lattice with basis $(0, \sqrt{3}a)$ and $(3a/2, \sqrt{3}a/2)$ in \mathbb{R}^2 , or a paving based on the truncated octahedron in $3D$ which is a standard representation of the alveolus [22]. Note that we will always use bold face to denote vectors or spaces of vectors.

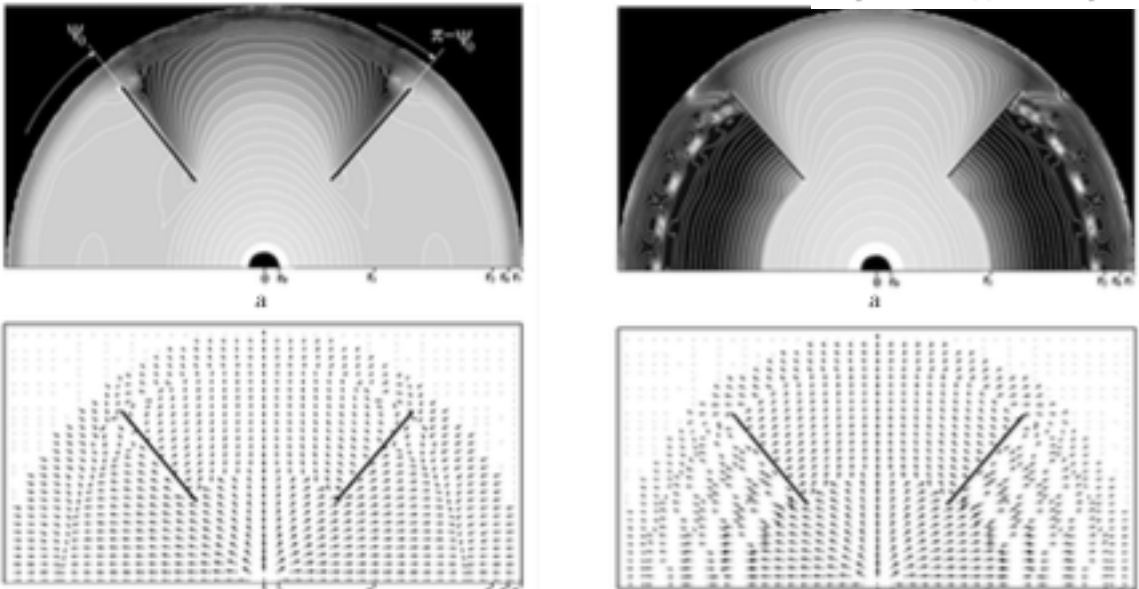


FIG. 4. (Color online) Geometry of the constructed airways: (a) Airway network 1, (b) airway network 2.

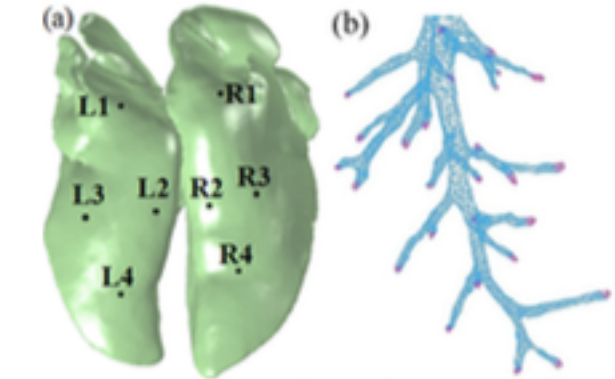
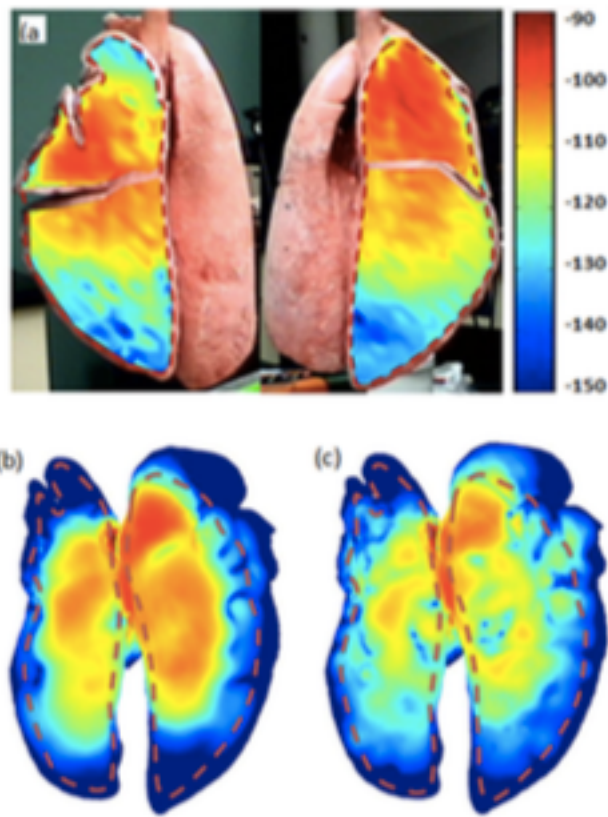


FIG. 6. (Color online) (a) Selected points on lung geometry for surface velocity amplitude comparison with experiment, (b) airway network 2 with terminal impedance specified.

Анализ литературы



For computational model evaluation, four points on each side of the lung were selected, and the surface velocity

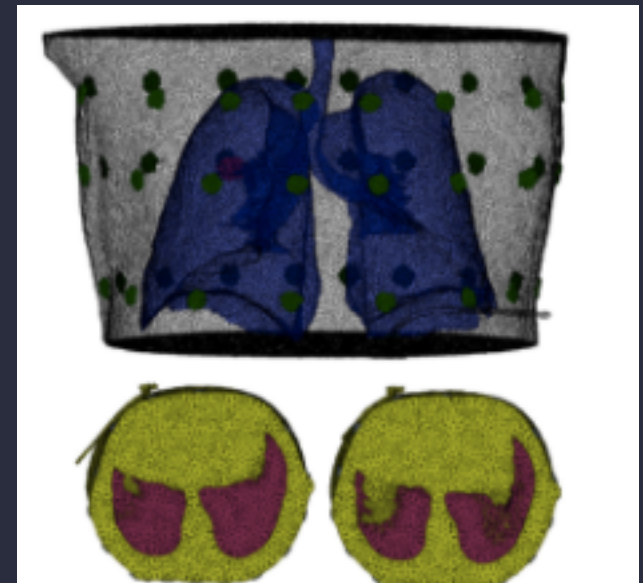
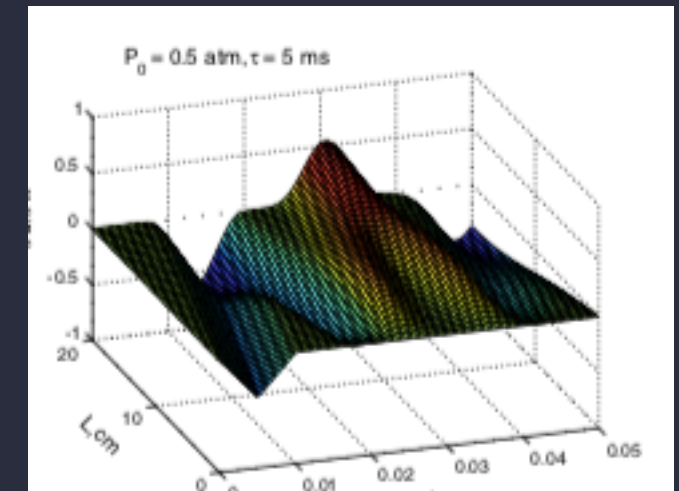
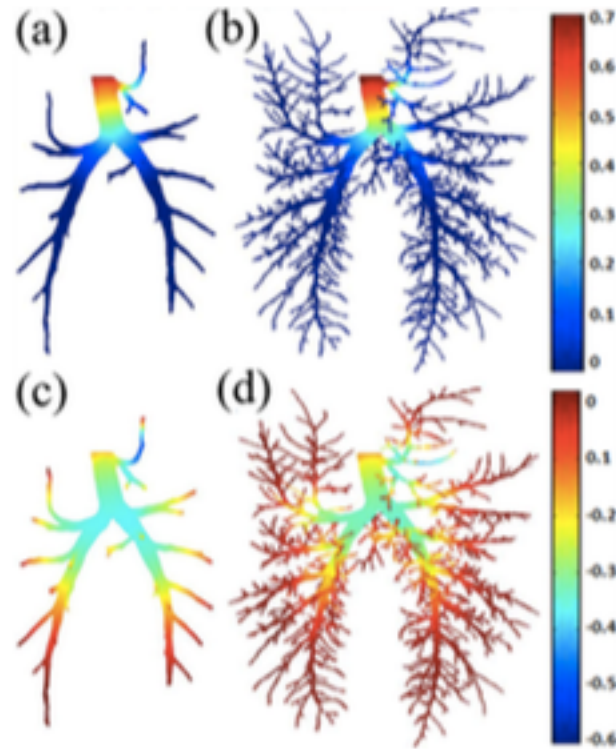
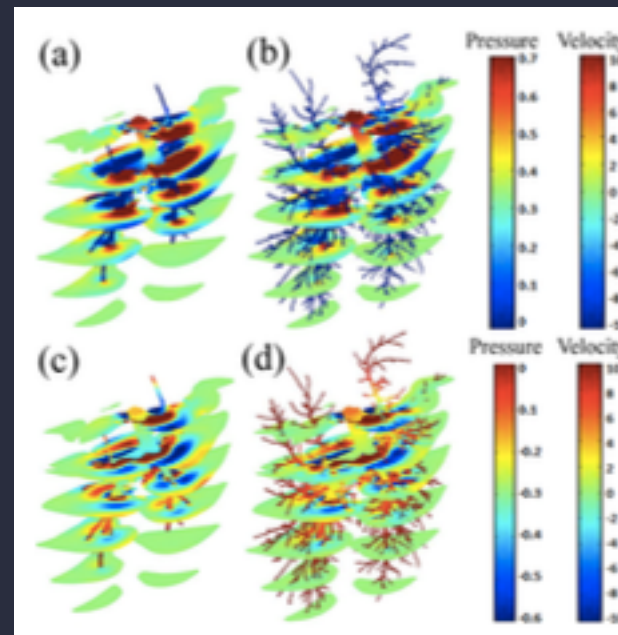
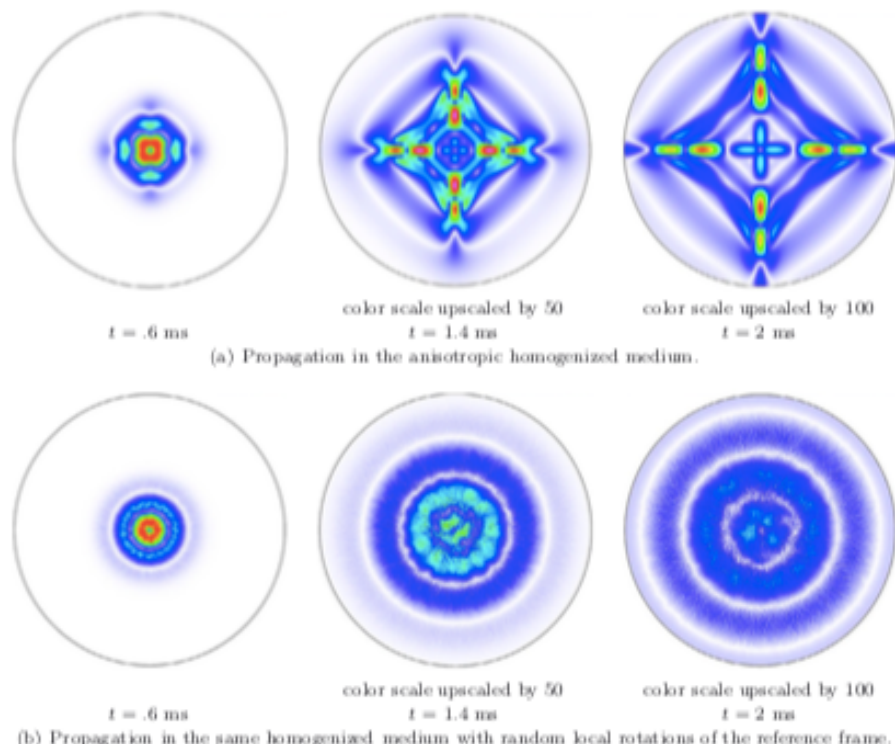


Figure 2: Fine FEM meshes of the human thorax. The top mesh shows the full mesh for the end inspiration instant. It contains 3 rings of 16 electrodes located two of them around the extremas of the lungs and the middle one in the tumour plane. The bottom meshes show the lowest electrode ring plane for end inspiration and end exhalation.

P. CAZEAUX AND J.S. HESTHAVEN



Математическая модель

Предположения

- среда ведет себя как жидкость (80% of body)
- среда неподвижна
- полное отражение на границах

Математическая модель

Волновое уравнение для неоднородной среды

$$\frac{1}{c^2(\mathbf{x})} \frac{\partial^2 p(\mathbf{x}, t)}{\partial t^2} = \rho(\mathbf{x}) \nabla \cdot \left(\frac{1}{\rho(\mathbf{x})} \nabla p(\mathbf{x}, t) \right),$$

$p(\mathbf{x}, t)$ - pressure, давление воздуха

$\rho(\mathbf{x})$ - плотность ткани / мышц

$c(\mathbf{x})$ - скорость звука

$\mathbf{x} = [x, y, z]$ | точка пространства

Математическая модель

Начальные условия

$$p(x, t=0) = 0 \text{ for all } x$$

$$\left. \frac{\partial p(x, t)}{\partial t} \right|_{t=0} = 0$$

Математическая модель

Начальные условия

$$p(x, t=0) = 0 \text{ for all } x$$

$$\left. \frac{\partial p(x, t)}{\partial t} \right|_{t=0} = 0$$

Граничные условия (отражения + границы пространства)

$$p(x, t) = 0 \text{ if } \rho(x) < 0.1 \text{ g/cc}$$

Математическая модель

Начальные условия

$$p(x, t=0) = 0 \text{ for all } x$$

$$\left. \frac{\partial p(x, t)}{\partial t} \right|_{t=0} = 0$$

Граничные условия (отражения + границы пространства)

$$p(x, t) = 0 \text{ if } \rho(x) < 0.1 \text{ g/cc}$$

Источник звука

$$p(a, b, c, t) = \sin(2\pi f t)$$

(a, b, c) - положение источника

Математическая модель

Численное приближ. решение

$$\begin{aligned} P_{i,j,k}^{m+1} = & (2 - 7.5\kappa_{i,j,k}^2)P_{i,j,k}^m - P_{i,j,k}^{m-1} \\ & + \frac{4\kappa_{i,j,k}^2}{3}[P_{i+1,j,k}^m + P_{i-1,j,k}^m + P_{i,j+1,k}^m + P_{i,j-1,k}^m + P_{i,j,k+1}^m + P_{i,j,k-1}^m] \\ & - \frac{\kappa_{i,j,k}^2}{12}[P_{i+2,j,k}^m + P_{i-2,j,k}^m + P_{i,j+2,k}^m + P_{i,j-2,k}^m + P_{i,j,k+2}^m + P_{i,j,k-2}^m] \\ & - \frac{\kappa_{i,j,k}^2}{3\rho_{i,j,k}}[(P_{i+1,j,k}^m - P_{i-1,j,k}^m) - (P_{i+2,j,k}^m + P_{i-2,j,k}^m)/8](\rho_{i+1,j,k} - \rho_{i-1,j,k}) \\ & - \frac{\kappa_{i,j,k}^2}{3\rho_{i,j,k}}[(P_{i,j+1,k}^m - P_{i,j-1,k}^m) - (P_{i,j+2,k}^m + P_{i,j-2,k}^m)/8](\rho_{i,j+1,k} - \rho_{i,j-1,k}) \\ & - \frac{\kappa_{i,j,k}^2}{3\rho_{i,j,k}}[(P_{i,j,k+1}^m - P_{i,j,k-1}^m) - (P_{i,j,k+2}^m + P_{i,j,k-2}^m)/8](\rho_{i,j,k+1} - \rho_{i,j,k-1}) \end{aligned}$$

$$\kappa_{i,j,k} = (l/h)c_{i,j,k}$$

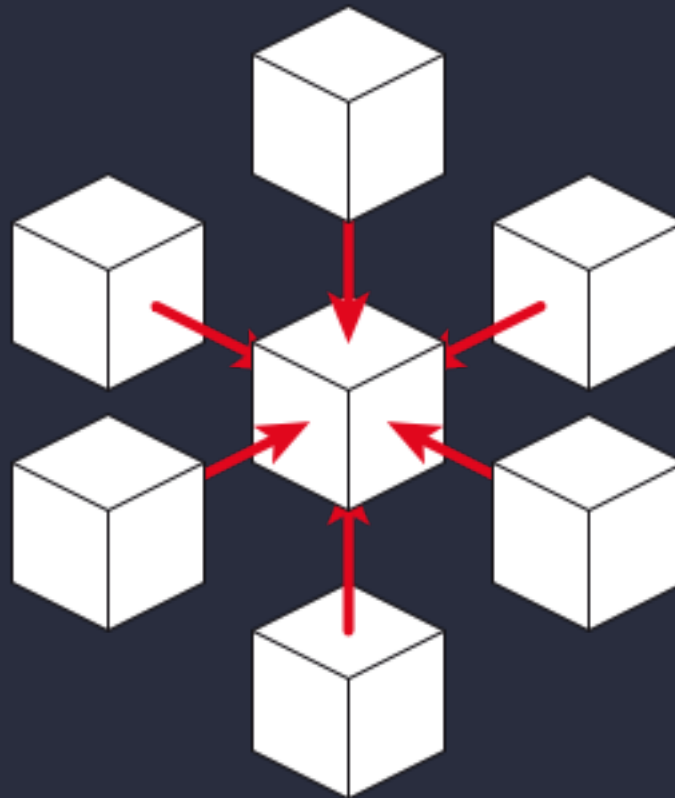
$$l = \Delta t$$

$$h = \Delta x = \Delta y = \Delta z$$

Метод конечных разностей, 7-point stencil
производные заменяются разностями

Математическая модель

7-point stencil method



$$\kappa_{i,j,k} = (l/h)c_{i,j,k}$$

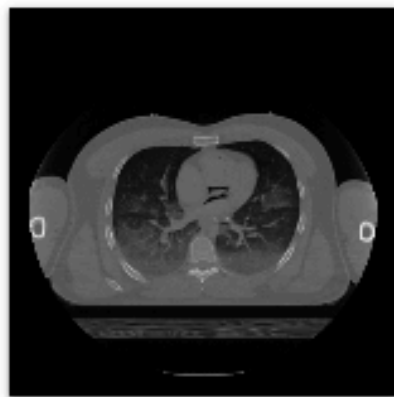
$$l = \Delta t$$

$$h = \Delta x = \Delta y = \Delta z$$

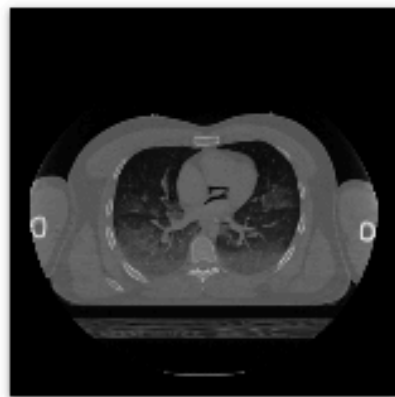
Численное приближ. решение.

Метод конечных разностей, 7-point stencil
производные заменяются разностями

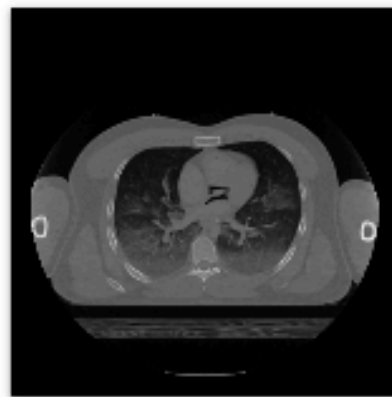
Human Visible Project Dataset



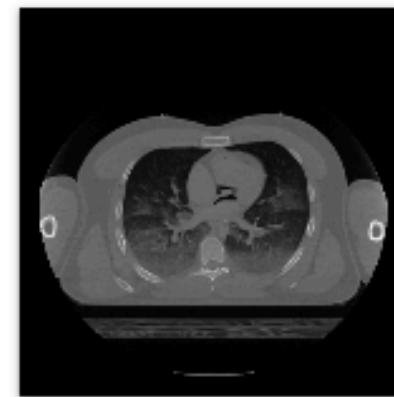
vhm.830.dcm.png



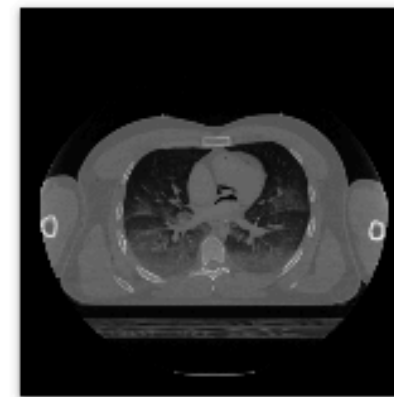
vhm.831.dcm.png



vhm.832.dcm.png



vhm.833.dcm.png



vhm.834.dcm.png



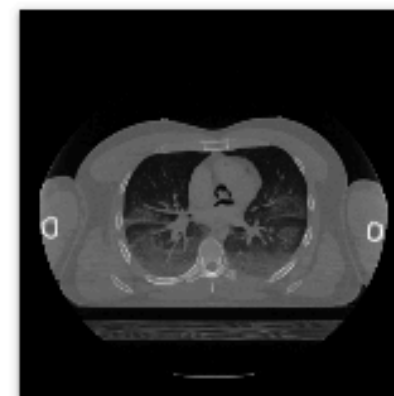
vhm.837.dcm.png



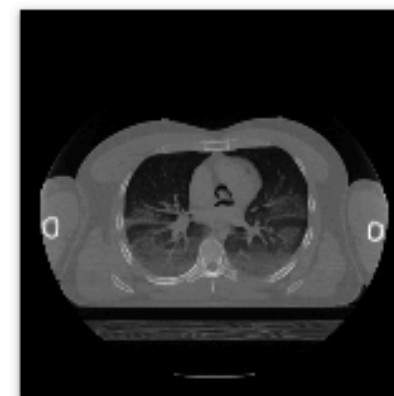
vhm.838.dcm.png



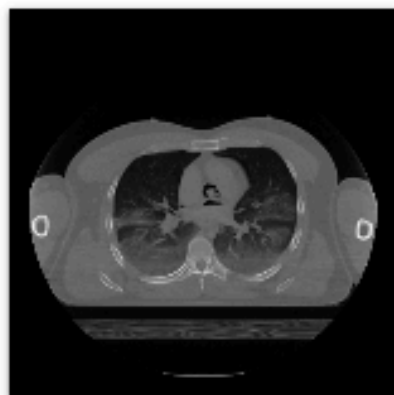
vhm.839.dcm.png



vhm.840.dcm.png



vhm.841.dcm.png



vhm.844.dcm.png



vhm.845.dcm.png



vhm.846.dcm.png

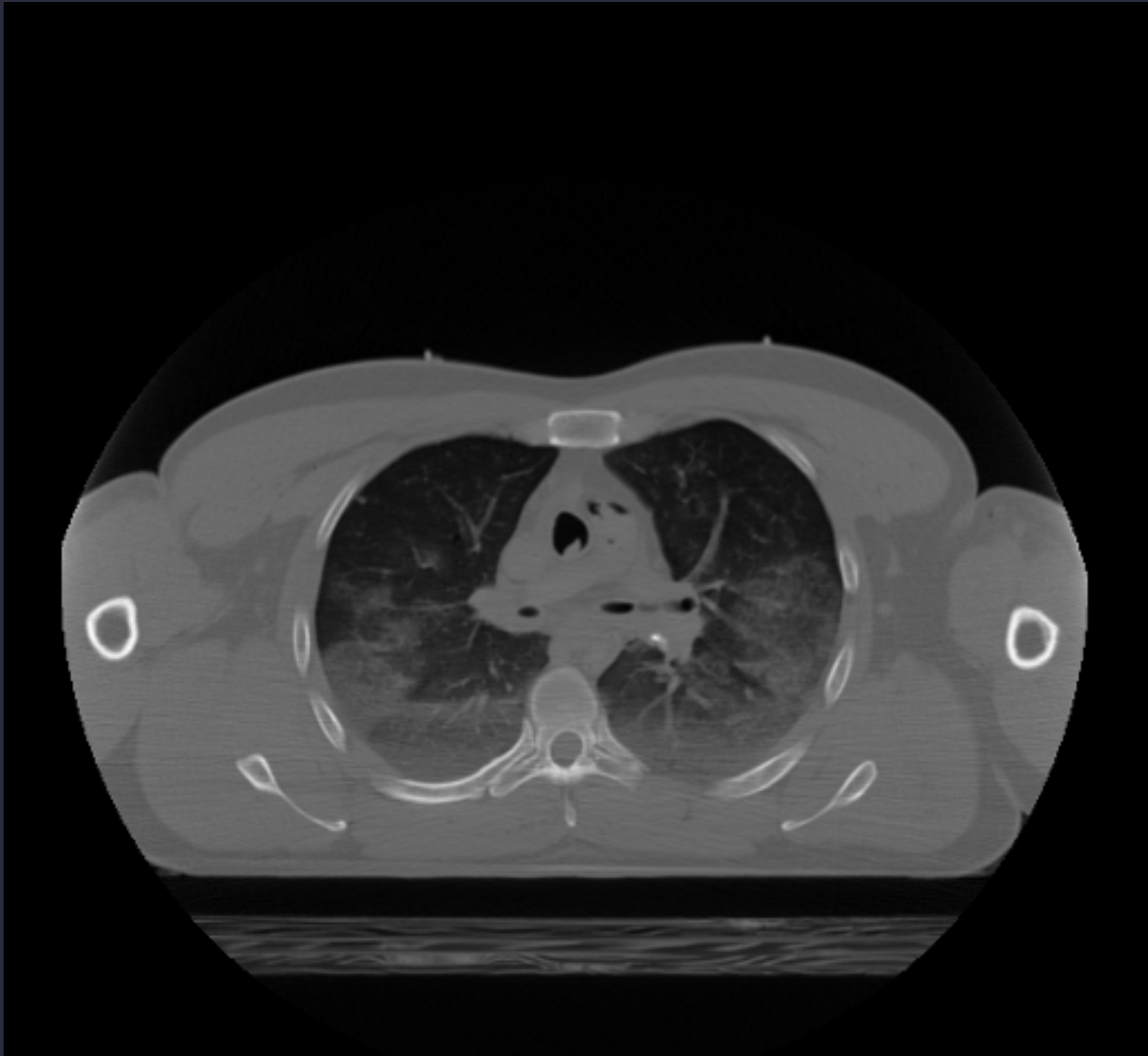


vhm.847.dcm.png



vhm.848.dcm.png

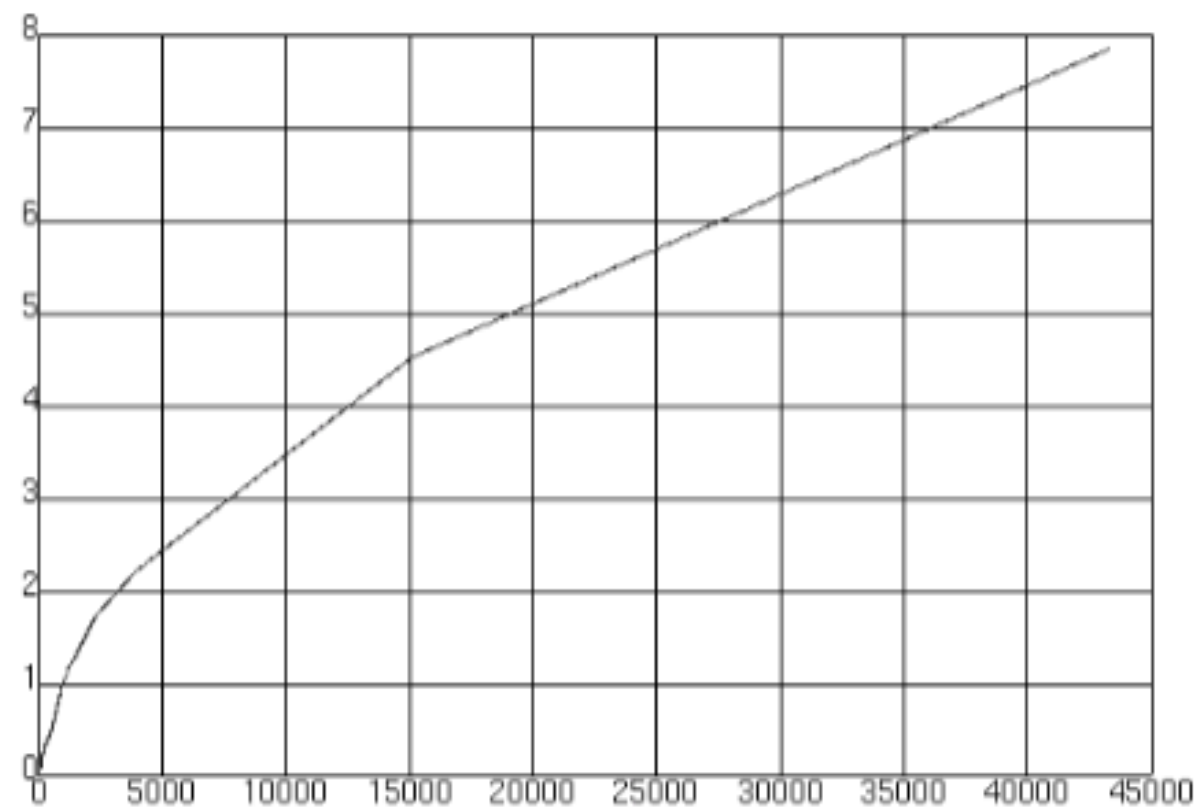
Human Visible Project Dataset



Human Visible Project Dataset



Human Visible Project Dataset



CT Number	Density
0	0.000
20	0.001
254	0.292
444	0.438
944	0.895
957	0.945
986	0.980
1024	1.000
1139	1.116
1211	1.142
1504	1.285
1884	1.473
2307	1.707
4000	2.213
15160	4.510
43410	7.850

Задачи работы

1. Анализ литературы
2. Основывать модель на реальных данных
3. Математическая модель
4. Компьютерная модель
5. Графический интерфейс для управления параметрами модели
6. Оптимизация модели для SIMD, GPU, CUDA
7. Изучение эффектов модели

Компьютерная модель

```
class LungsModel():
    l_default = 0.065
    h_default = 0.55e-6
    f_default = 110
    # l_default = 0.1
    # h_default = 1
    # f_default = 440

    def __init__(self, L=l_default, H=h_default, F=f_default): ...

    def update_P(self):
        """
        mb work with flat and then reshape in return
        norm by now, mb add some more optimisations in future, also cuda
        """

        S = self.P_p.shape[0]
        N = self.P_p.shape[1]

        self.P[2:-2, 2:-2, 2:-2] = 2 * self.P_p[2:-2, 2:-2, 2:-2] - self.P_pp[2:-2, 2:-2, 2:-2]

        Z = np.zeros_like(self.P_p)
        Z[2:-2, 2:-2, 2:-2] = 22.5 * self.P_p[2:-2, 2:-2, 2:-2]

        cell_indecies_flat = np.arange(S * N * N).reshape(S, N, N)[2:-2, 2:-2, 2:-2].ravel().reshape(-1, 1) # vertical vector

        s1_indexes_flat = cell_indecies_flat + np.array([-1, 1, -N, N, -N**2, N**2]) # i±1 j±1 k±1
        s2_indexes_flat = cell_indecies_flat + np.array([-1, 1, -N, N, -N**2, N**2]) * 2 # i±2 j±2 k±2
        s1_values = self.P_p.ravel()[s1_indexes_flat] # each row contains 6 neighbors of cell
        s2_values = self.P_p.ravel()[s2_indexes_flat] # each row contains 6 neighbors of cell
        s1 = np.sum(s1_values, axis=1) # sum by axis=1 is faster for default order
        s2 = np.sum(s2_values, axis=1)

        Z[2:-2, 2:-2, 2:-2] -= 4 * s1.reshape(S-4, N-4, N-4)
        Z[2:-2, 2:-2, 2:-2] += 1/4 * s2.reshape(S-4, N-4, N-4)

        m1 = np.array([1, -1, -1/8, -1/8])
        m2 = np.array([1, -1])

        s3_V_indexes = cell_indecies_flat + np.array([N**2, -N**2, 2*N**2, -2*N**2])
        s3_V_values = self.P_p.ravel()[s3_V_indexes] * m1 # по идее можно за скобки как то винести m1 и m2
        s3_V_sum = np.sum(s3_V_values, axis=1)
```

Задачи работы

1. Анализ литературы
2. Основывать модель на реальных данных
3. Математическая модель
4. Компьютерная модель
5. Графический интерфейс для управления параметрами модели
6. Оптимизация модели для SIMD, GPU, CUDA
7. Изучение эффектов модели